

# Late Quaternary fault activity in the Western Carpathians: evidence from the Vikartovce Fault (Slovakia)

RASTISLAV VOJTKO<sup>1\*</sup>, FRANTIŠEK MARKO<sup>1</sup>, FRANK PREUSSER<sup>2</sup>, JÁN MADARÁS<sup>3,4</sup> and MARIANNA KOVÁČOVÁ<sup>1</sup>

<sup>1</sup>Department of Geology and Paleontology, Faculty of Natural Sciences, Comenius University, Mlynská dolina G, 842 15 Bratislava, Slovak Republic; \*vojtko@fns.uniba.sk;

<sup>2</sup>Department of Physical Geography and Quaternary Geology, Stockholm University, 10691 Stockholm, Sweden

<sup>3</sup>Dionýz Štúr State Institute of Geology, Mlynská dolina 1, 817 04 Bratislava, Slovak Republic

<sup>4</sup>Geophysical Institute, Slovak Academy of Sciences, Dúbravská cesta 9, 845 28 Bratislava, Slovak Republic

(Manuscript received September 6, 2010; accepted in revised form June 9, 2011)

**Abstract:** The Cenozoic structure of the Western Carpathians is strongly controlled by faults. The E-W striking Vikartovce fault is one of the most distinctive dislocations in the region, evident by its geological structure and terrain morphology. This feature has been assumed to be a Quaternary reactivated fault according to many attributes such as its perfect linearity, faceted slopes, the distribution of travertines along the fault, and also its apparent prominent influence on the drainage network. The neotectonic character of the fault is documented herein by morphotectonic studies, longitudinal and transverse valley profile analyses, terrace system analysis, and mountain front sinuosity. Late Pleistocene activity of the Vikartovce fault is now proven by luminescence dating of fault-cut and uplifted alluvial sediments, presently located on the crest of the tilted block. These sediments must slightly pre-date the age of river redirection. Considering the results of both luminescence dating and palynological analyses, the change of river course probably occurred during the final phase of the Riss Glaciation ( $135 \pm 14$  ka). The normal displacement along the fault during the Late Quaternary has been estimated to about 105–135 m, resulting in an average slip rate of at least  $0.8\text{--}1.0 \text{ mm} \cdot \text{yr}^{-1}$ . The present results identify the Vikartovce fault as one of the youngest active faults in the Central Western Carpathians.

**Key words:** Western Carpathians, Vikartovce fault, Quaternary faulting, luminescence dating, neotectonics, tilting.

## Introduction

The Pliocene–Quaternary relief evolution of the Central Western Carpathians has been investigated since the middle of the 20<sup>th</sup> century when the role of faults in morphological structures was recognized (Mičian 1962; Lukniš 1964; Mazúr 1965; Dzurovčín 1994). The study area is located in the northern part of the region formed by the Kozie Chrbty Mountains and the Hornád Depression. The boundary between the Kozie Chrbty Mts and the Paleogene Hornád Depression is morphologically distinct, perfectly linear, and it is represented by the Vikartovce fault (VIF), which is located at the southern foot of the Kozie Chrbty Mts (Figs. 1, 2). The VIF has been identified as one of the most distinctive and important young faults of the Western Carpathians, responsible for the creation of the near-by graben and horst structures. The fault was regarded as a neotectonically active dislocation (Roth 1938; Lukniš 1973; Maglay et al. 1999), due to distinctive morphological expressions of the fault trace, fault related distribution of Quaternary travertine, change of river courses and capturing due to fault activity. However, a part of the scientific community remained sceptical about a tectonic origin of the upper reach of the Hornád Valley, rather interpreting this structure as a narrow bay of the Paleogene sediments within the paleo-Alpine nappe units (Gross et al. 1999b).

At present, the VIF is considered to be a neotectonic dislocation, but no exact data concerning the age are known yet. According to this hypothesis, the paleo-rivers flowing north-

wards were disrupted by the Vikartovce fault, along which the Kozie Chrbty Mts emerged and formed a barrier for these rivers. This led to the change in the drainage network system. The original directions of flows were interrupted and rivers at the southern foot of the uplifted Kozie Chrbty Mts turned to the east.

The main goal of this paper is to review the available knowledge and to summarize the authors' arguments concerning the neotectonic nature and properties of the VIF. To solve this topic, a multidisciplinary approach was applied strongly focused on field investigations. Analysis of structures, sediments, and landforms appears to be an efficient tool to detect young faulting. The landforms of the area were evaluated by field observations and by morphostructural analysis of digital terrain models (DTM). This paper uses a DTM and associated software (GRASS-GIS) to prepare set of maps and morphostructural parameters revealing the orientation of topographical features. This allows identification of structural features (e.g. main joint sets, fault scarps or landslide scarps) that are involved in rock slope instabilities. Optically Stimulated Luminescence (OSL) and Infrared Stimulated Luminescence (IRSL) were used to date the age of the VIF activity, and so test whether block tilting was the reason for change in the drainage network. We sampled buried alluvial sediments, which were formed by ancient river flow, later disrupted by the VIF and uplifted, now being preserved on a dry saddle highly elevated above the present river course. From this setting, it is expected that the age of the alluvial deposits just pre-



**Fig. 1.** Shaded elevation map of central Slovakia. The location of the study area is shown by a black polygon.

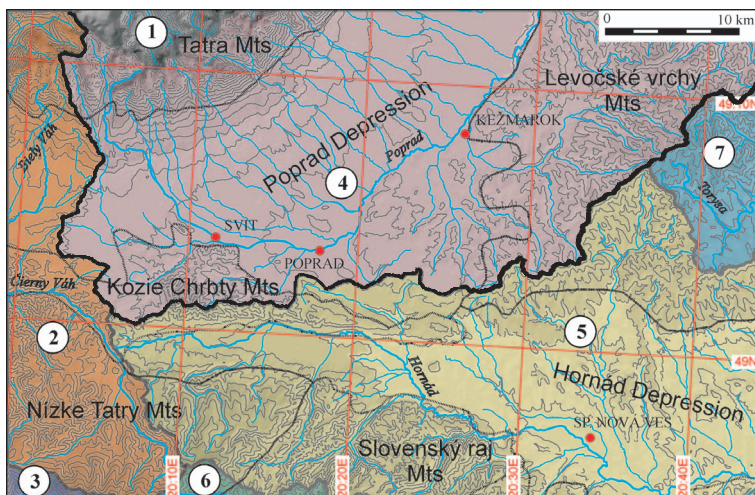


**Fig. 2.** Map of the geomorphological units and recent river catchments. Explanation: 1 — The Dunajec, 2 — the Váh, 3 — the Hron, 4 — the Poprad, 5 — the Hornád, 6 — the Hnilec, 7 — the Torysa drainage basins. Black line represents the main watershed in Central Europe; the northern part belongs to the Baltic Sea and the southern part to the Black Sea Basin. Dotted lines are boundaries between geomorphological units presented herein.

dates river interruption and gives the maximum age of the latest activity of the VIF.

## General overview

### Geological and tectonic setting

The study area belongs to the Central Western Carpathians (cf. Plašienka et al. 1997; Plašienka 1999). The Kozie Chrby and Nízke Tatry Mountains are formed by the Boca Nappe, which belongs to the Hronic Unit (Fig. 3). It is composed of a Late Paleozoic volcano-sedimentary succession (Ipolitca

Group) and Triassic, predominantly carbonatic rocks (Vozárová & Vozár 1988). The south-eastern part of the investigated area (Slovenský Raj Mountains) is composed of the Silicic Unit which consists predominantly of Triassic carbonatic rocks with typical Wetterstein (Middle Triassic) and Dachstein (Upper Triassic) formations (Biely et al. 1992, 1997; Mello et al. 2000a,b).

The paleo-Alpine nappes form the basement of the Eocene to Oligocene sedimentation of the Hornád Depression (Fig. 3). Structurally, this basin belongs to the Central Carpathian Paleogene Basin (CCPB) which was formed as a marginal sea of the Peri-Tethyan Basin. It shows a fore-arc basin position developed on the destructive plate margin and behind the Outer Carpathian accretionary wedge (Soták et al. 2001). The time span of this sedimentary succession is expected to be Lutetian to latest Oligocene/Early Miocene according to nannoplankton evidence (Soták et al. 1996; Soták 1998; Olszewska & Wiczeorek 1998).

The Quaternary deposits are found mainly on the Paleogene formations of the Central Carpathian Paleogene Basin. The spatial distribution and sediment thickness of the Quaternary deposits is highly variable, due to landforms and local variability of sedimentary processes during the Late Pleistocene to Holocene (Fig. 3). The most common Quaternary deposits are lithologically undivided slope sediments, representing polygenic fine-grained sediments, sporadically bearing rubble (Gross et al. 1999a,b). Predominant occurrence of these sediments is recorded in flat relief positions on flysch formations, with a prevailing content of claystones. Their thickness often exceeds 2 m (Biely et al. 1997; Mello et al. 2000b). Late Pleistocene and Holocene fluvial deposits are located mainly along the Hornád River.

Pleistocene to Holocene travertines are predominantly situated near Poprad and form individual mounds (Fig. 3). The largest travertine mounds in the Central Western Carpathians are also located in the eastern continuation of the VIF in the surrounding of Spiš Castle.

### Geomorphological setting and drainage systems

The investigated area is located in the northern part of the region, with a typical morphostructural pattern of substituting heights and depressions (Figs. 1, 2). The Kozie Chrby Mts and the Hornád Depression are elongated in the E-W direction and have a very narrow shape. The Kozie Chrby Mts are rimmed by the Hornád Depression to the south and by the Poprad Depression to the north.

The watershed between the Poprad and Hornád Rivers has already drawn the attention of previous research, indicating that the study area was notably influenced by reorganization of the river network and drainage basin formation during the

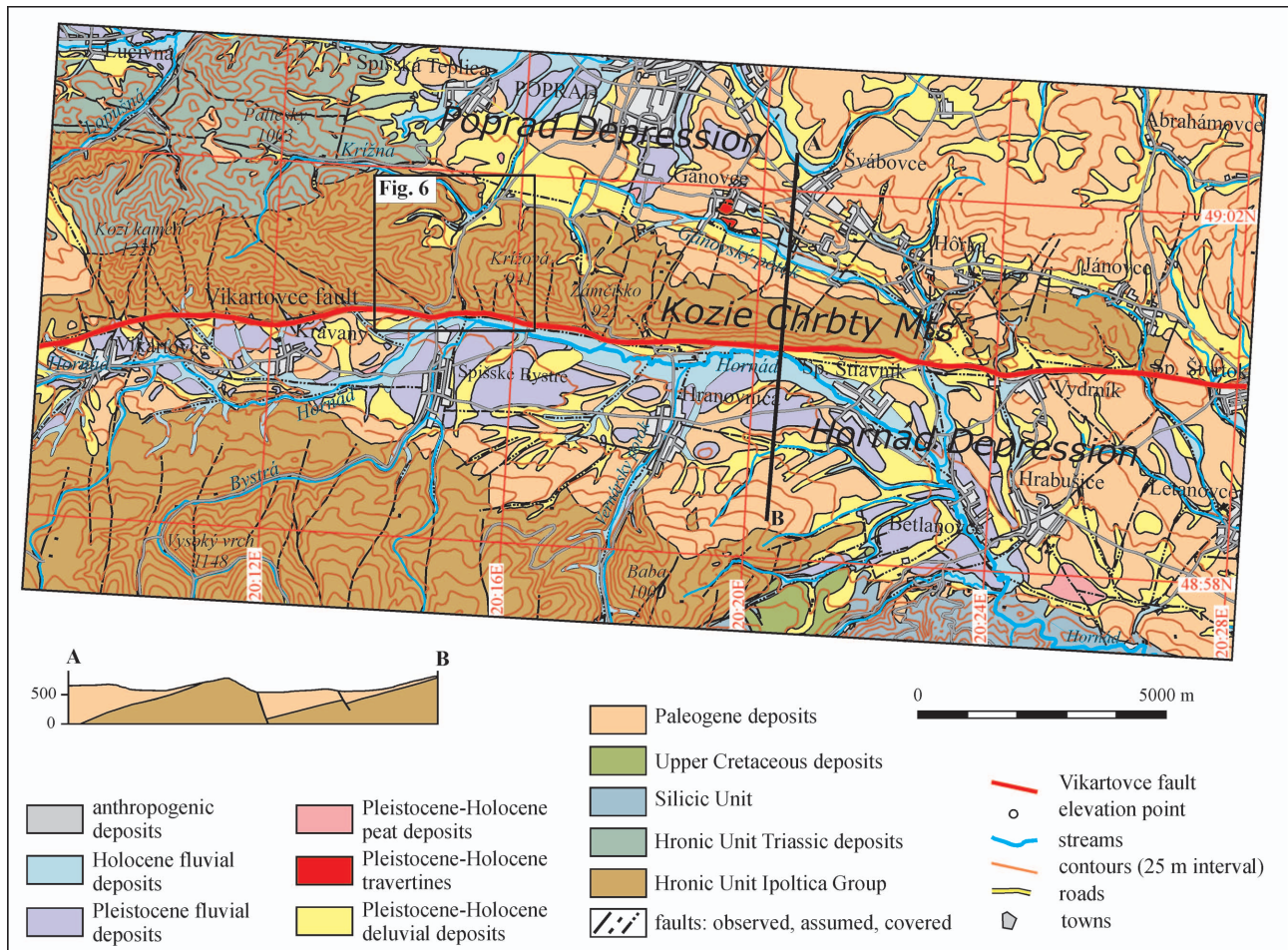


**Fig. 3.** Simplified geological map with geological cross-section without Quaternary deposits (modified according to Biely et al. 1992; Gross et al. 1999a; Mello et al. 2000a).

Quaternary (cf. Roth 1938; Lukniš 1973). Currently, the Kozie Chrbty Mts, which are a relatively insignificant mountain chain, form part of the main watershed in Central Europe between the Poprad drainage basin (Vistula River system) belonging to the Baltic Sea Basin, and the Hornád drainage basin (Tisa and Danube river system) belonging to the Black Sea Basin (Fig. 2). The presence of remains of fluvial gravel on the top of the Kozie Chrbty Mts implies that streams (paleo-Hornád River and Vernársky potok Stream), originating from the Nízke Tatry Mountains flowed across the structure (Roth 1938; Lukniš 1973).

## Research methods

### Field geological research and drilling

The Quaternary deposits preserved in the deep seated saddles of the Kozie Chrbty horst were mapped in the field using a 5 m contour interval topographic map at a scale of 1:10,000. This mapping was supported by the interpretation of aerial ortho-photographs and DTM at a scale of 1:10,000, with a cell size of 5 m. According to the results of the field

geological research, sites for drilling were selected. A drill diameter size of 20 cm was used to recover cores that are suitable to be used for luminescence dating. Three boreholes were drilled with drilling depths of 7 (V-1), 12 (V-2), and 22 meters (V-3) respectively. The cores were logged with regard to their sedimentological properties.

### Source maps, data and GIS applications

Radar data and 3D visualization were used for identification and description of map-scale structures and for establishing a terrain shape digital model. A DTM was derived from vectorized contours of topographic maps at a scale of 1:10,000 with a cell size of 5 m. For a broader view, the DTM was based on Shuttle Radar Topography Mission (SRTM) with spatial resolution three-arc-second (Jarvis et al. 2008). Topographic, longitudinal, and transverse river valley profiles were also constructed on these DTM based raster maps.

Information from geological maps at a scale of 1:50,000 (Biely et al. 1992; Gross et al. 1999a; Mello et al. 2000b) and 1:200,000 (Polák et al. 2008; Mello et al. 2008) was cross-checked with new observations in the most relevant parts of the study area.

### *Elevation, slope and drainage network*

The altitude, slope, and aspect were modelled and used for morphometric analysis. These parameters were computed using GRASS-GIS software (GRASS Development Team, 2010). The GRASS-GIS software calculates the orientation of each cell of the DTM using regularized spline with tension method for approximation from vector data using the *v.surf.rst* from vectorized contours of the maps at a scale of 1 : 10,000. The module does not require input data with topology, therefore both level 1 (no topology) and level 2 (with topology) vector point data are supported. Additional points are used for approximation between each two points on a line if the distance between them is greater than specified *dmax*. If *dmax* is small (less than cell size) the number of added data points can be very large and slow down approximation significantly. The implementation has a segmentation procedure based on quad-trees which enhances the efficiency for large data sets (GRASS Development Team 2010).

Morphometric parameters are computed directly from the approximation function so that the important relationships between these parameters are preserved. The equations for computation of these parameters and their interpretation are fully described in Mitašová & Mitaš (1993) and Mitašová & Hofierka (1993). Slope angles are computed in degrees (0–90).

The derivation of the drainage basins was carried out by the *r.watershed* module of the GRASS-GIS software by defining the critical source area with the threshold using the parameters of *basin* and *half.basin* (Kinner et al. 2005; GRASS Development Team 2010). The selection of an adequate threshold was crucial, because it defines the dimensions of the valleys to be analysed. The threshold represents the minimum size of an exterior watershed basin in cells when no flow map is available for input, or overland flow units when there is a flow map. Accordingly, for the recognition of systematic drainage features indicative of neotectonic deformation, a qualitative analysis of the drainage pattern was also essential (Delcaillau 2001; Schumm et al. 2002).

### *Mountain front sinuosity*

The mountain front is especially defined by the value of the change of slope inclination. The linearity of the mountain front was quantified by a slightly reinterpreted *S* index (Bull & McFadden 1977):

$$S = L_{mf} \cdot L_s^{-1},$$

where  $L_{mf}$  is the total length of the considered segment of the mountain front and  $L_s$  is the length of abscissa between the start and end points of the considered segment of mountain front. The  $L_s$  value reflects the real course of the fault system on which the mountain front was developed. An *S* value approaching 1.0 indicates a very linear mountain front which points towards young deformational activity along the frontal structures. Higher values indicate a degraded mountain front, which results from tectonic inactivity (interconnected with weathering conditions) or extremely fast weathering processes. However, Bull & McFadden (1977) originally developed the *S* index for straight mountain fronts. As tilted

and rotated blocks of various volumes are common in the Western Carpathians, this produces complex fault systems, hence not straight but often curved patterns. As a consequence, the use of  $L_s$  values in a traditional way may produce incorrect results and we therefore experimented with tuning the  $L_s$  values. There are high prepositions, that the fault system limits well preserved facets and underlying flat base surfaces. Therefore we used the idealized mountain front defined by the flow-line, which delimits the lower facet's  $L$  edges (cf. Vojtko et al. 2011).

### *Normalized longitudinal valley profiles and stream gradient*

Generally, a fluvial system reacts to tectonic influences by changing its longitudinal and transverse river profiles, its channel pattern, and/or its sediment discharge. Longitudinal and transverse river profiles were constructed based on the DTM with cell sizes of 5×5 meters.

The longitudinal river profiles were analysed as most commonly practised (Hack 1973; Demoulin 1998; Wobus et al. 2006). Their quantified parameters are used to compare different drainage systems, and specifically, to identify the response of neotectonic activities in the drainage basins. Data were obtained from the DTM using the GRASS-GIS module *r.drain* which traces a flow through a minimum grid value path in a DTM.

Normalized longitudinal river profiles were applied to describe the geomorphic response of rivers in regions with active tectonics (Zuchiewicz 1991, 1998; Demoulin 1998; Ruzkiczay-Rüdiger et al. 2009). The advantage of these profiles is the direct comparison of valleys with different lengths and absolute gradients because they are dimensionless (Fig. 4). The abscissa is  $d/D$ , where  $D$  is the profile length and  $d$  is the distance of the individual data points from the stream source at one end of the profile. The ordinate represents the normalized elevation to the absolute gradient along the valley ( $e/E$ ) where  $E$  is the absolute elevation ( $E = E_{max} - E_{min}$ ) and  $e$  is the elevation of individual data points along the profile. Normalized profiles characterize the degree of grading of a river where  $z_{max}$  is the maximal concavity, and  $\Delta d/D$  is the normalized distance of  $z_{max}$  from the source (Fig. 4). The area on the plot between the valley profile and the straight line connecting the source and the outlet of the valley is the concavity index  $\sigma$  in percent. Theoretically, this index lies between 0.0 (0 %) and 0.5 (100 %). Higher values indicate a more concave profile, or a more highly graded river (Demoulin 1998; Molin et al. 2004; Ruzkiczay-Rüdiger et al. 2009).

The stream gradient (SG) was calculated for successive 100-m-long segments along the stream. The sensitivity of the SG to changes in the channel slope makes it possible to evaluate the relationships between tectonic activity, rock resistance, and topography.

### *Luminescence dating*

Luminescence allows the dating of the last daylight exposure of quartz and feldspar grains using a latent light-sensitive signal within the minerals that is erased during sediment transport. During burial, when the grains are sealed from daylight,

the latent luminescence signal is induced within the minerals by the interaction of ionizing radiation with the crystal lattice. Detailed reviews of the methodology have recently been provided by, for example, Wintle (2008) and Preusser et al. (2008, 2009). For age calculation, two values have to be determined, the amount of radiation dose absorbed and stored as latent luminescence signal by the mineral ( $D_e$ ) and the dose rate ( $D$ ), which means the amount of radiation dose per year.

For this study, material recovered by coring was transferred to the luminescence laboratories in Bern and the outer 5 cm, contaminated during the coring process and potentially exposed to daylight, were removed. Sediment from the inner part was prepared for  $D_e$  determination applying standard chemical pre-treatments (HCl,  $H_2O_2$ , Na-oxalate) followed by density separation (LST Fast Flow<sup>®</sup> with densities of  $2.70 \text{ g}\cdot\text{cm}^{-3}$  and  $2.58 \text{ g}\cdot\text{cm}^{-3}$ ). The quartz fraction was etched with 40% HF for one hour, rinsed with demineralized water, and subsequently treated with HCl to remove fluorites. Small aliquots (2 mm) were used for  $D_e$  determination applying modified versions of the Single-Aliquot Regenerative dose (SAR) protocol (cf. Murray & Wintle 2000; Wintle & Murray 2006). The purity of quartz separates was routinely checked by exposure to IR diodes and aliquots showing a significant IR response were rejected from  $D_e$  determination.  $D_e$  was calculated using Optically Stimulated Luminescence (OSL) from quartz (60 s stimulation at  $125^\circ\text{C}$ ) and Infrared Stimulated Luminescence (IRSL) from feldspar (300 s stimulation at  $30^\circ\text{C}$ ). Preheating at  $230^\circ$  for 10 s (quartz) and  $290^\circ$  for 10 s (K-feldspar) prior to all luminescence measurements was done according to the results of standard performance tests (dose recovery, thermal transfer). No evidence for anomalous fading in K-feldspar was observed in storage tests. The shape of quartz OSL decay curves of samples VIF1 and VIF2 indicates strong presences of medium components reported to cause significant age shortfall (Steffen et al. 2009). For the

lower part of the sequences, we interpret the IRSL ages as probably reflecting the real deposition age of the samples and the apparent OSL ages for this part are actually inconsistent with stratigraphy and the rest of the dating results.

Dose rates were determined using low-level high-resolution gamma spectrometry (cf. Preusser & Kasper 2001). Equilibrium of the decay chain of  $^{238}\text{U}$  was investigated using the approaches described in Preusser & Degering (2007) and Zander et al. (2007). While samples VIF1 and VIF2 are likely in equilibrium, the other two samples show some weak evidence for open system behaviour, namely a loss of  $^{238}\text{U}$  in VIF3 and a gain of  $^{238}\text{U}$  in VIF4. However, this is regarded as having a negligible effect on age determination.

## Results

### Geological and geomorphological survey

The Kozie Chrbty Mts are oriented in an E-W direction with a length of more than 20 km and a width ranging from 1 to 5 km. Elevations ( $E$ ) within the study area vary between 417 and 1259 m a.s.l., with the average altitude approximately 740 m a.s.l. The slope map enhances the general E-W oriented geomorphic features such as the Kozie Chrbty Mts and the Hornád Basin (Fig. 5).

In the Vysová pass, a system of degradational terraces is very well preserved (Fig. 6). The terrace system of the ancient Hornád River is located on the eastern slopes of Kozí Kameň Mount and the western slopes of the Křížová Mount at a higher elevation than the Vysová pass. The older terraces than the flattened surface of the Vysová pass are arranged into four levels with preserved gravel remnants. These remnants are composed predominantly of Upper Permian sandstones, diabase, basalt pebbles of the Hronic Unit, and also Paleogene sandstones of the Central Carpathian Paleogene Basin. The younger terraces belong to the modern Hornád River alluvial sediments on the Vysová pass. This terrace system is located predominantly on the southern slope of the Kozie Chrbty Mts horst and it is not well-developed due to high basal erosion during and after the VIF activity.

### Mountain front sinuosity

In context of the morphotectonic pattern, the VIF is represented especially by contrast relief landforms (facet slopes vs. flat surfaces). This fault is also associated with the southern mountain front of the Kozie Chrbty horst. The  $S$  index reaches from 1.05 to 1.07 within the study area (Fig. 5). This is close to the value of 1.0 which expresses the identity of the low-destructed and real mountain front line. The fact that the actual mountain front is low-destructed by exogenic processes refers to a considerable role of very young tectonics in the shaping of these contrast relief landforms.

### Longitudinal valley profiles and stream gradients

Normalized longitudinal river profiles (Fig. 7) and their concavity parameters were computed to identify vertical de-

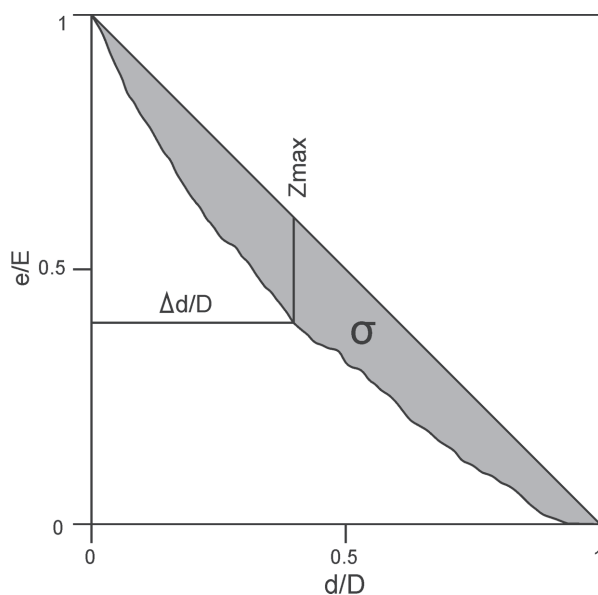


**Fig. 4.** Normalized longitudinal river valley profiles. Further explanation see in the text.

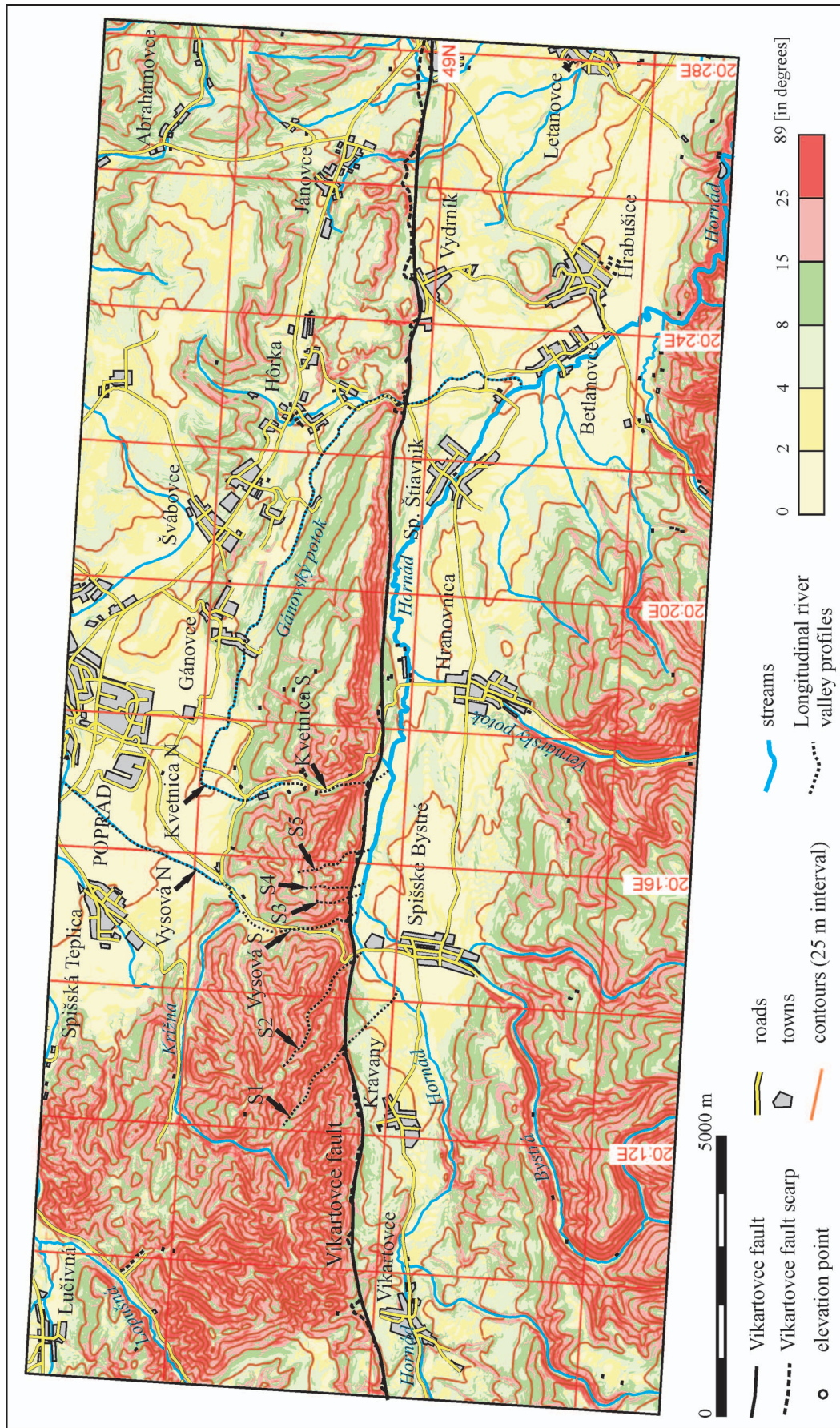
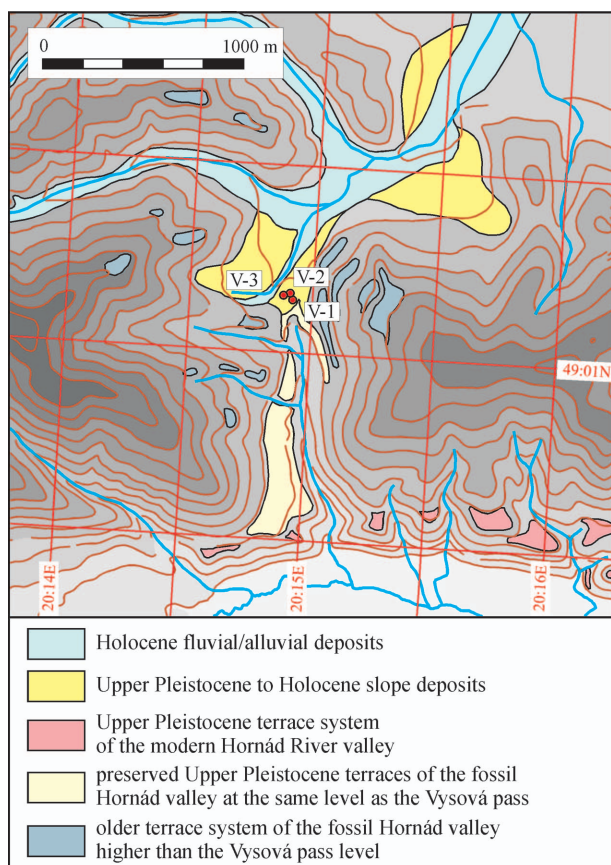


Fig. 5. Slope map with principal geomorphological units and location of analysed longitudinal river valley profiles. The slopes were computed using DTM with the intervals. The trace of the Vikartovce fault is shown by black solid and mountain front sinuosity by black dashed lines.



**Fig. 6.** Map of the Pleistocene terrace system in the Vysová pass neighbourhood with the location of the boreholes.

formations and state of stream development affecting the drainage network of the study area. Therefore, a total of nine longitudinal river profiles were analysed and their location is shown in Fig. 5. The maximum concavities ( $z_{max}$ ) are 0.10–0.31 for the Stream #2 and Kvetnica S stream respectively, and their positions are very irregular which depends on the type of valley and azimuthal orientation. The ratio  $\Delta d/D$  was computed from 0.22–0.82 for the Stream #2 and Vysová S stream respectively. The concavity index  $\sigma$  varies from 6.52 for the Vysová S to 28.18 for the Vysová N streams. The analysed streams in the study area belong to the Hornád drainage basin except the Vysová N stream which belongs to the Poprad drainage basin (Fig. 2). These streams can be divided into two groups based on computed  $\Delta d/D$ ,  $z_{max}$  and  $\sigma$  parameters from the normalized longitudinal river profiles (Table 1).

The streams that flow from the Kozie Chrbty horst towards the south are characterized by small concavity with  $\sigma$  varying from 6.52 to 24.79, and very variable  $\Delta d/D$  and  $z_{max}$  parameters (Table 1). These streams also have complicated shapes on the graphs of the longitudinal river profiles (Fig. 7). The lower parts of the river profiles are generally concave in shape, which then changes increasingly to convex towards the head of the stream. Finally, the upper parts have also concave shape. The knick-points in the longitudinal river profiles regularly appear approximately 150–250 m

upstream from the foothill and indicate young tectonic activity along the southern margin of the Kozie Chrbty horst (Fig. 7). The lowermost and the uppermost courses are generally well-graded, unlike the middle parts of the streams, which are evidently influenced by vertical movements of terrain blocks along the VIF.

Stream gradients of valleys located on the southern side of the Kozie Chrbty Mountains are more curved and reach values greater than 14 (Fig. 8). Interestingly, the stream gradient curves are almost identical. The maximum stream gradient is generally located 150–250 m from the southern mountain front of the Kozie Chrbty horst. In contrast, the upper courses of the streams are characterized by low gradients generally not exceeding 7.5.

The longitudinal river profile of the Kvetnica N is very specific because the stream flows from the Kozie Chrbty horst towards the north and then rapidly changes its flow direction towards the east and south-east. The upper reach belongs to a paleo-stream and the central and lower parts of the valley are evidently affected by river piracy which is recorded by its complicated shape (Figs. 7, 8).

The Vysová N stream is the second stream that flows towards the north and can be characterized as a graded stream with the highest  $\sigma = 28.18$ , quite high  $\Delta d/D$  and  $z_{max}$  parameters (*sensu* Mackin 1948). This stream has a characteristic concave upward profile and it was not influenced by active faulting during the Quaternary Period. The ancient valley located north of the Vysová pass is influenced by river capture and at present it is characterized by a very low stream gradient which does not exceed a value of 7 (Fig. 8). The whole upper reach of this valley has a very low stream gradient (less than 5), but the lower part near the confluence with the Poprad River is already affected by headward erosion after reorganization of the river network (Lacika 1998). The main valleys on the northern side of the mountain are affected by lateral erosion. The shape of the valleys is more open than the previous ones and the valleys are significantly filled by slope sediments derived from the slopes along the valleys. The thickness of slope sediment reaches up to 13 m, as in the Vysová pass (Fig. 8).

**Table 1:** Morphometric parameters of normalized longitudinal valley profiles in the Kozie Chrbty horst. Explanations: **Name** — name of analysed profiles, **D** — total distance from the source to confluence with the Hornád or Poprad rivers, **E** — absolute gradient, **Gr** — relative gradient (E/D),  $z_{max}$  — maximal concavity,  $\Delta d/D$  — distance of  $z_{max}$  from the source and  $\sigma$  — concavity index. Note, location of streams is shown in Fig. 5.

No.	Name	D [m]	E [m]	Gr [m/km]	$z_{max}$	$\Delta d/D$	$\sigma$ [%]
1	Kvetnica N	14773	204	13.82	0.28	0.42	28.12
2	Kvetnica S	1697	142	83.92	0.31	0.62	22.45
3	Stream 1	3521	334	94.83	0.16	0.50	20.32
4	Stream 2	2775	323	116.24	0.10	0.22	14.15
5	Stream 3	1035	39	37.31	0.24	0.74	24.79
6	Stream 4	1118	54	48.52	0.20	0.78	16.04
7	Stream 5	1327	102	76.77	0.17	0.31	17.38
8	Stream 6	1600	77	48.24	0.21	0.40	27.09
9	Vysová N	6296	76	12.00	0.23	0.35	28.18
10	Vysová S	1542	114	73.72	0.11	0.82	6.52

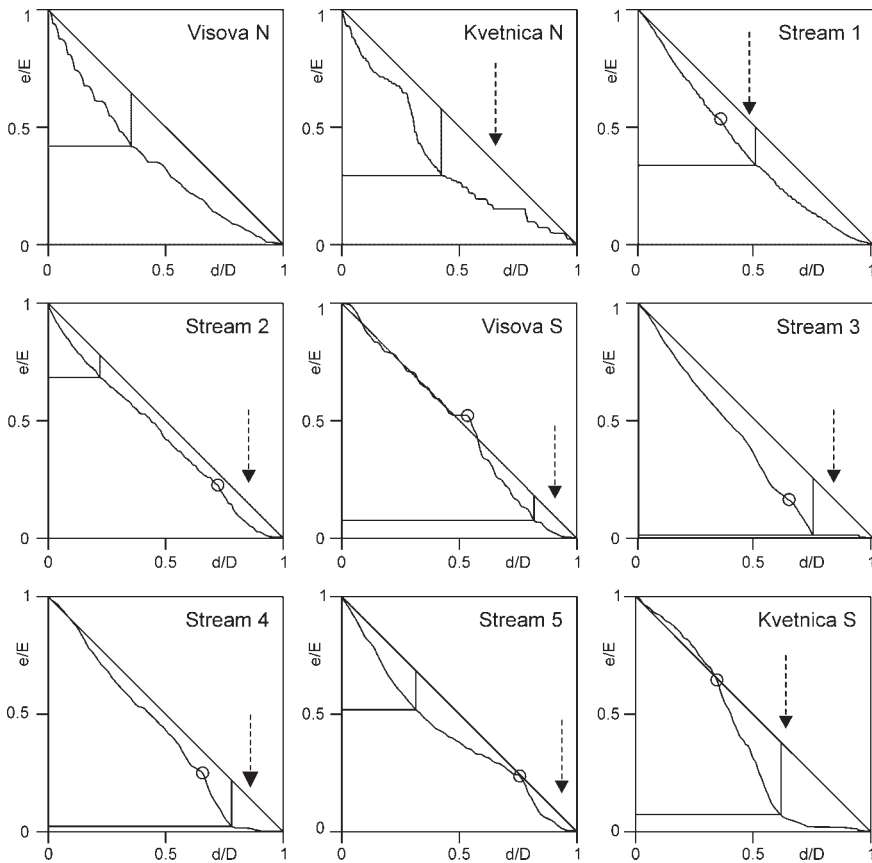


Fig. 7. ▲

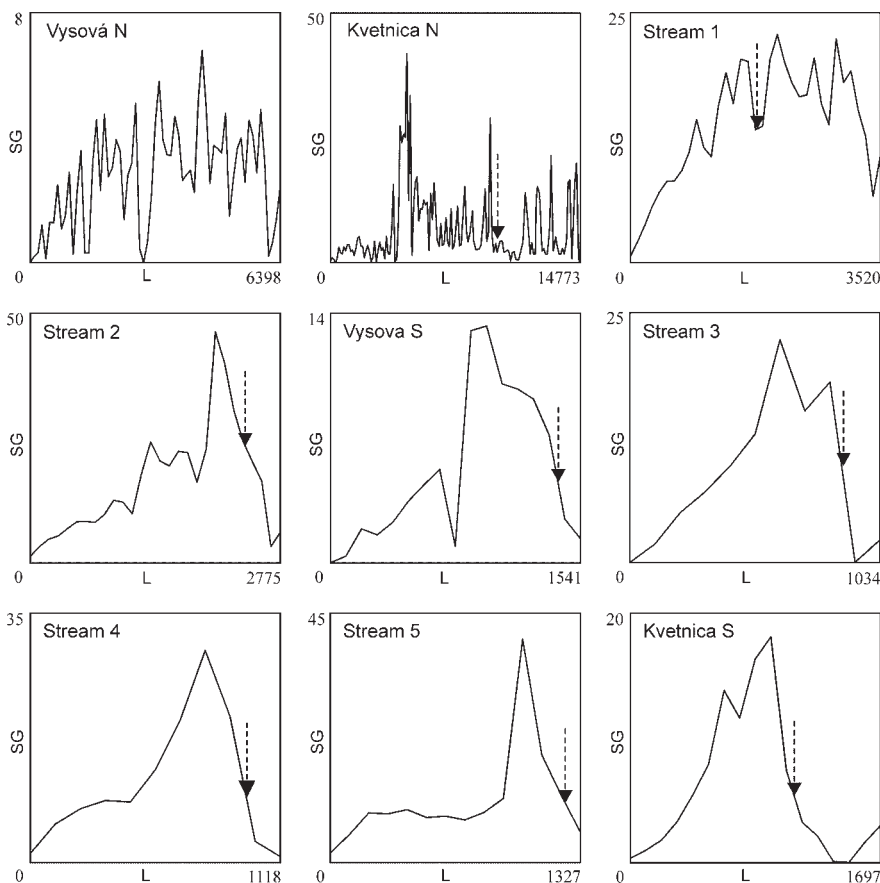


Fig. 8. ▼

### Age of the Vikartovce fault activity

According to our hypothesis, the alluvial sediments which were preserved in the Vysová pass can date the VIF tectonic activity. The fluvial sediments were first described from the Poprad brick-yard, north of the Kozie Chrbty Mts (Lukniš 1973). From the lithology of these river sediments its source area was in the Nízke Tatry Mts, indicating a north-bound transport. Recently no river or stream of this course exists on the northern slope of the horst with the capacity to transport the described alluvial deposits. This is an important argument to support the barrier/tilting model described above. The age of alluvial sediments deposited by the former river probably dates the age of river interruption, which simultaneously slightly pre-dates the age of the VIF Quaternary activity.

Due to recultivation, the old brick-yard disappeared and extensive urbanization in the area of Poprad town did not allow any surveys. However, following the observations by Roth (1938) and Lukniš (1973), we expected alluvial sediments of a former N-S river flowing cross-cutting the Kozie Chrbty horst at the presently dry Vysová pass (Fig. 6).

Based on evidence from geological field investigation and geophysical profiling, three shallow boreholes (V-1, V-2, and V-3) were drilled to sample the alluvial sediments. The third borehole (V-3) was used for sampling (Fig. 6). It penetrated brownish/yellowish sandy loam (slope sediments) in the upper part of the profile at a depth of 0.0–12.8 m and a sequence of grey sands intercalated by clays and pebble clays at a

**Fig. 7.** Normalized longitudinal river valley profiles. The position of the Vikartovce fault is indicated by arrows and main knick-points by circle.

**Fig. 8.** Stream gradients. The abscissa is L—the profile length in meters and the ordinate represents stream gradient (SG) in meters for successive 100-m-long segments along the stream. The position of the Vikartovce fault is indicated by arrows.

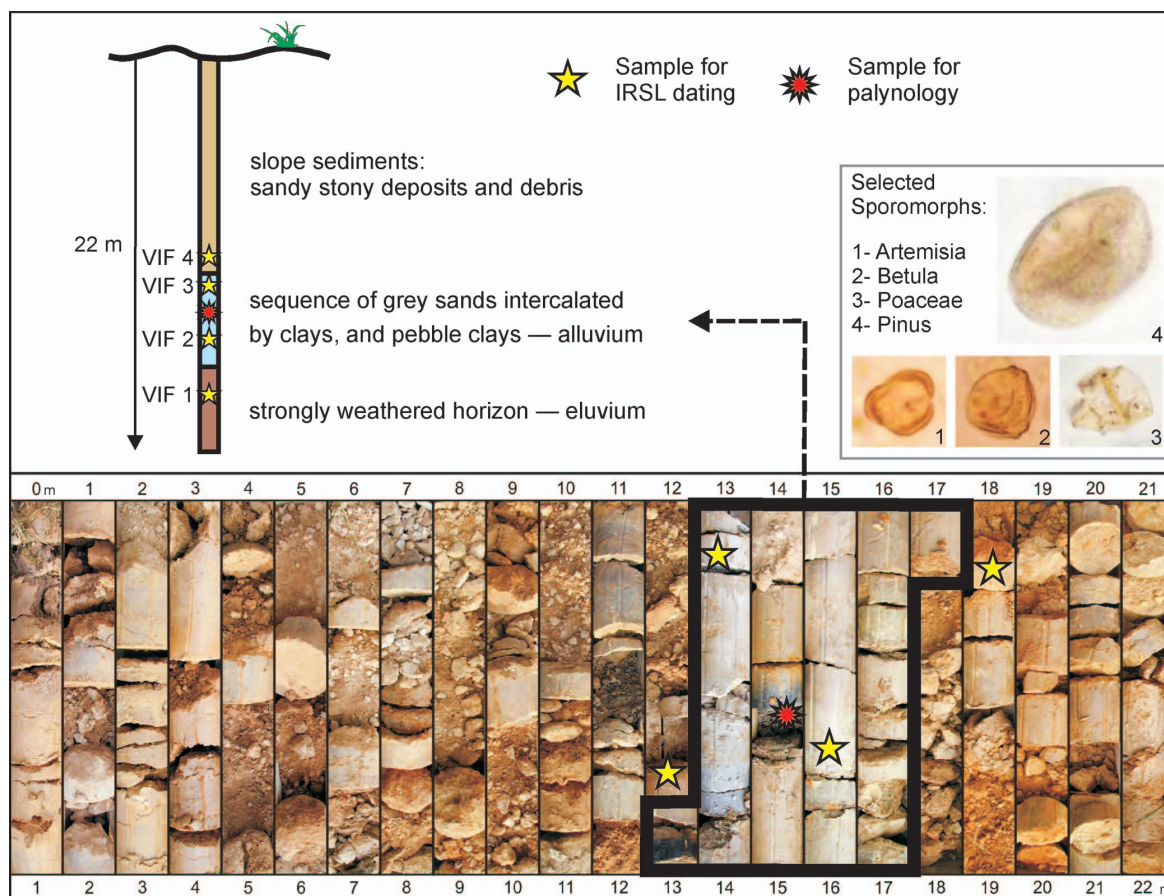


Fig. 9. The V-3 drill log with indications of sampling points, location and palynological analyses of alluvial horizon.

depth of 12.8–17.2 m. The lower portion of the profile, under alluvial deposits at a depth of 17.2–22 m, represents a strongly weathered horizon of eluvial deposits (Fig. 9). This weathered horizon comprises numerous bedrock clasts but the borehole did not penetrate the bedrock itself.

Samples for OSL/IRSL dating were taken from the top of the weathered horizon (VIF1: 18.2 m), the alluvial sediments (VIF2: 15.7 m, VIF3: 13.2 m), and the lowermost part of overlying slope sediments (VIF4: 12.7 m). As stated above, the OSL ages for the two lower samples are considered unreliable.

The age for material from the weathered horizon, probably representing input from slope processes, is dated to  $167 \pm 11$  ka (IRSL). Ages for the alluvial sediments are (Table 2):  $135 \pm 14$  ka (IRSL),  $143 \pm 9$  ka (IRSL), and  $114 \pm 9$  ka (OSL).

In addition to luminescence dating, palynological analyses of the alluvial horizon were carried out. The sample was selected from a thin (17 cm) intercalation of dark grey clay inside the alluvial horizon at a depth of 14.5 m (Fig. 9). The most frequent taxa in the analysed clay horizon represent herbs (*Artemisia*, Asteraceae, Chenopodiaceae) and a small

**Table 2:** Summary of luminescence data giving the grain size investigated, the number of replicate measurements for  $D_e$  determination ( $n$ ), the concentration of dose rate relevant elements  $K$ ,  $Th$ , and  $U$  (1 = as determined for  $^{238}U$  from 186 keV line, 2 = mean of  $^{214}Pb$  and  $^{214}Bi$  lines),  $W$  = water content used for dose rate calculation, sampling depth below present surface, dose rate ( $D$ ) calculated using  $U$  (2), mean  $D_e$ , and resulting IRSL (feldspar) and OSL (quartz) age. \* — Quartz OSL ages are significantly underestimated due to the presence of a strong medium component in the signal.

Sample	Grain size [μm]	n	K [%]	Th [ppm]	U (1) [ppm]	U (2) [ppm]	W [%]	Depth [m]	D [Gy·ka <sup>-1</sup> ]	D <sub>e</sub> [Gy]	Age [ka]
VIF4F	200–250	15	1.80 ± 0.07	4.76 ± 0.07	0.80 ± 0.33	1.08 ± 0.01	15 ± 5	12.5	2.82 ± 0.17	494.2 ± 9.0	175 ± 11
VIF4Q	200–250	15	1.80 ± 0.07	4.76 ± 0.07	0.80 ± 0.33	1.08 ± 0.01	15 ± 5	12.5	2.00 ± 0.16	255.0 ± 18.2	128 ± 13
VIF3F	200–250	15	1.60 ± 0.07	5.54 ± 0.26	1.81 ± 0.50	1.17 ± 0.06	15 ± 5	13.0	2.73 ± 0.18	369.2 ± 29.9	135 ± 14
VIF3Q	200–250	15	1.60 ± 0.07	5.54 ± 0.26	1.17 ± 0.06	1.17 ± 0.06	15 ± 5	13.0	1.90 ± 0.13	215.4 ± 5.5	114 ± 9
VIF2F	200–250	15	2.33 ± 0.09	7.37 ± 0.08	1.55 ± 0.46	1.57 ± 0.01	15 ± 5	16.7	3.50 ± 0.21	500.5 ± 10.4	143 ± 9
VIF2Q	200–250	3	2.33 ± 0.09	7.37 ± 0.08	1.57 ± 0.01	1.57 ± 0.01	15 ± 5	16.7	2.67 ± 0.18	184.1 ± 20.6	69 ± 9 *
VIF1F	200–250	15	1.99 ± 0.08	6.68 ± 0.24	1.32 ± 0.64	1.42 ± 0.05	15 ± 5	18.0	3.12 ± 0.14	524.6 ± 10.9	167 ± 11
VIF1Q	200–250	3	1.99 ± 0.08	6.68 ± 0.24	1.42 ± 0.05	1.42 ± 0.05	15 ± 5	18.0	2.31 ± 0.17	110.7 ± 26.5	48 ± 12 *

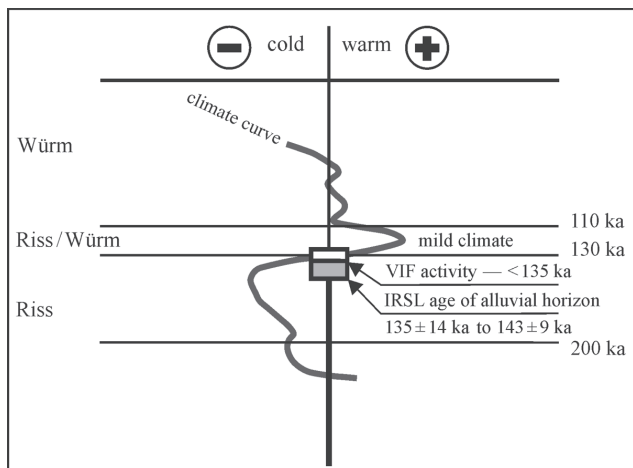


**Fig. 10.** IRSL age span of fossil river sediments and the related age of the VIF activity triggering in comparison with climate curve (after Gibbard & Cohen 2008) corresponding to the described palyno-taxa assemblage (Fig. 9).

proportion of *Pinus* and *Betula* is also recorded. This assemblage points towards an open landscape without forest (Lang 1994; Jankovská et al. 2002). The vegetation recorded in this sediment, especially the presence of *Betula nana*, high values of *Artemisia* and Poaceae indicate rather cool climatic conditions (Fig. 9).

### Interpretation

The Vikartovce fault (VIF) is interpreted as normal fault system with dipping of the fault plane southward. The total slip along the Vikartovce fault for the period ca. 135 ka to present is approximately given by the difference in altitude between the top of the Rissian deposits on the pass and the Hornád alluvial plain. It is estimated to 105–135 m. Please note that this is only the vertical slip along the fault and that the horizontal component of movement is currently not known. Using these data, the average movement along the VIF is between 0.8 and 1.0 mm·yr<sup>-1</sup>. In the Western Carpathians, a velocity of vertical movements of approximately 1 mm a year during the Quaternary Period was also confirmed in the area of Turiec Basin (Kováč et al. 2011) and the Horná Nitra Basin (Vojtko et al. 2011) based on sedimentological and morphostructural data. Recent faulting is attended by seismic activity recorded by historical and contemporary earthquakes in the study area (Cipcjar et al. 2009).

The erosional rate for the last 135 ka was not estimated because of lack of any relevant data. Several small and at least one principal knick-points along the individual longitudinal river profiles in the southern part of the Kozie Chrby Mts support irregular movement along the VIF fault. This implies that the active movement occurred only occasionally and it was separated by periods of fault inactivity. Unfortunately, there are no data available with regard to the frequency of active faulting. However, some indications were observed such as knick-points on longitudinal river valley profiles.

The regular knick-points are distinct along the whole mountain boundary and they are interpreted as degraded fault scarps during the last higher tectonic activity (younger than 135 ka). Generally, the computed values of the southern streams imply active movement of the Vikartovce fault. Deviations from the graded longitudinal river profiles are indicative of external influences, especially neotectonic activity as is expected here (Holbrook & Schumm 1999; Gelabert et al. 2005).

The most likely mechanism for the horst origin was block tilting, where the VIF operated as a boundary normal fault of the tilted block (Kozie Chrby horst). An argument supporting this interpretation is the observed asymmetry of the horst, which is typical of tilted blocks. The northern slopes of the horst are low angle, while the southern slopes are steep, representing more or less the Vikartovce fault scarp. We expect that the VIF itself is steeply dipping to the south as well.

The lower age limit for river redirection, and as a consequence the maximum age of fault triggering, is given by these ages. For the slope sediments, post-dating this event, the OSL age of 128 ± 13 ka is consistent with the age estimates of the alluvial sediments, while the IRSL age of 175 ± 11 ka is apparently overestimated (Table 2).

In combination with the results from luminescence dating, the deposition of the fluvial sediments is correlated to the transition from the Riss Glaciation towards the Last Interglacial (Eemian), that is sometime around 135 ka (Figs. 9, 10). This age most probably pre-dates the Pleistocene activity of the VIF.

### Conclusions

The morphotectonic, geological, sedimentological, structural, and geochronological evidence for the Quaternary activity of the Vikartovce fault has been summarized here. The Kozie Chrby horst has a distinct morphological asymmetry, where the southern slopes along the VIF are steep and the northern slope is generally flat (Fig. 5). The normalized longitudinal profiles show principal knick-points on curves which are considered to be retreated fault scarps after the last higher movement of the VIF. The knick-points are located approximately 150–250 m north of the present VIF trace (Fig. 7). Moreover, the differences between stream gradient on the southern (high gradient) and northern (low gradient) valleys of the Kozie Chrby horst is conspicuous (Fig. 8). This asymmetric pattern is caused by VIF activity and block tilting.

The most expressive argument of the Vikartovce fault Quaternary activity is the change of the drainage network due to fault-related block separation. Fossil rivers originally flowing from the south to the north were disrupted by the Vikartovce fault, and then fault controlled tilting created a barrier — an asymmetric horst, what led to the change in rivers course from the S-N to W-E (Fig. 5). Luminescence dating was used for the first time in the Slovak Carpathians, indicating that alluvial sediments deposited by the fault-cut fossil river have an age of around 135 ka (Table 2). It categorizes the Vikartovce fault to the youngest confirmed dislocation in the Western Carpathians. During the late stages of the Quaternary, the fault has been activated as a very dynam-

ical structure, and it declares the Late Pleistocene fault separation. The vertical separation along the fault for this stage has been estimated as 105–135 m.

The speed of movement (computed only for vertical component) along the Vikartovce fault ranges between 0.8 and 1.0 mm·yr<sup>-1</sup>, calculated as average speed which is equal to total distance covered divided by total time required. Anyway, slip rates from 1 to 2 mm·yr<sup>-1</sup> might be considered average for major, active faults (Yeats et al. 1997). All mentioned properties of the VIF are typical for active faulting with seismic capability. Figuring out the rate of slip along faults is a key to understanding the relative “importance” of faults in an area, and the geological and seismic hazard those faults present to local residents and developments.

**Acknowledgments:** This work was supported by the Slovak Research and Development Agency under the contract No. APVV-0158-06. We are grateful to Dr. Kamil Ustaszewski and Dr. Herfried Madritsch who inspired and encouraged us to carry out luminescence dating in our research. We also thank Dr. Herfried Madritsch, Prof. Klaus Reicherter and Dr. Jozef Vozár for the detailed reviews of this paper and constructive comments.

## References

- Biely A., Beňuška P., Bezák V., Bujnovský A., Halouzka R., Ivanička J., Kohút M., Klíneč A., Lukáčik E., Maglay J., Miko O., Pulec M., Putiš M. & Vozár J. 1992: Geological map of the Nízke Tatry Mountains. *Geological Institute of Dionýz Štúr*, Bratislava.
- Biely A., Bujnovský A., Vozárová A., Klíneč A., Miko O., Halouzka R., Vozár J., Beňuška P., Bezák V., Hanzel V., Kubeš P., Lukáčik E., Maglay J., Molák B., Pulec M., Putiš M. & Slavkay M. 1997: Explanation to Geological Map of the Nízke Tatry Mts (1:50,000). *State Geol. Inst. Dionýz Štúr*, Bratislava, 1–232 (in Slovak).
- Bull W.B. & McFadden L.D. 1977: Tectonic geomorphology north and south of the Garlock Fault, California. In: Doehring D.O. (Ed.): *Geomorphology in arid regions*. *State Univ. New York at Binghamton*, Binghamton, 115–138.
- Cipciar A., Fojtíková L., Bystrický E., Kristeková M., Franek P., Gális M., Kristek J., Moczo P. & Pažák P. 2009: Slovak earthquakes catalogue. *Slovak Acad. Sci.*, Bratislava.
- Delcaillau B. 2001: Geomorphic response to growing fault-related folds: example from the foothills of central Taiwan. *Geodinamica Acta* 14, 265–287.
- Demoulin A. 1998: Testing the tectonic significance of some parameters of longitudinal river profiles: the case of the Ardenne (Belgium, NW Europe). *Geomorphology* 24, 189–208.
- Dzurovčín L. 1994: Contribution to the identification of the processes and progress of the planation in the Slovak Carpathians: their relation to the neotectonic phases and paleogeographical evolution in the Paratethys. *Miner. Slovaca* 26, 2, 126–143 (in Slovak).
- Gelabert B., Fornós J.J., Pardo J.E., Rosselló M.V. & Segura F. 2005: Structurally controlled drainage basin development in the south of Menorca (Western Mediterranean, Spain). *Geomorphology* 65, 139–155.
- Gibbard P.L. & Cohen K.M. 2008: Global chronostratigraphical correlation table for the last 2.7 Million years. *Episodes* 31, 2, 243–247.
- GRASS Development Team 2010: Geographic Resources Analysis Support System (GRASS) Software, Version 6.4.0. <http://grass.osgeo.org>
- Gross P., Buček S., Ďurkovič T., Filo I., Karoli S., Maglay J., Nagy A., Halouzka R., Spišák Z., Žec B., Vozár J., Borza V., Lukáčik E., Mello J., Polák M. & Janočko J. 1999a: Geological map of Popradská kotlina Basin, Hornádska kotlina Basin, Levočské vrchy Mts, Spišsko-šarišské medzihorie Depression, Bachureň Mts and Šarišská vrchovina highland (scale 1:50,000). *Ministry of Environment of Slovak Republic, Geol. Surv. Slovak Republic*, Bratislava.
- Gross P., Buček S., Ďurkovič T., Filo I., Maglay J., Halouzka R., Karoli S., Nagy A., Spišák Z., Žec B., Vozár J., Borza V., Lukáčik E., Janočko J., Jetel J., Kubeš P., Kováčik M., Žáková E., Mello J., Polák M., Siráňová Z., Samuel O., Snopková P., Raková J., Zlinská A., Vozárová A. & Žecová K. 1999b: Explanation to Geological map of Popradská kotlina Basin, Hornádska kotlina Basin, Levočské vrchy Mts, Spišsko-šarišské medzihorie Depression, Bachureň Mts and Šarišská vrchovina highland (scale 1:50,000). *Ministry of Environment of Slovak Republic, Geol. Surv. Slovak Republic*, Bratislava, 1–239 (in Slovak).
- Hack J.T. 1973: Stream profile analysis and stream gradient index. *U.S. Geol. Surv. J. Res.* 1, 4, 421–429.
- Holbrook J. & Schumm S.A. 1999: Geomorphic and sedimentary response of rivers to tectonic deformation: a brief review and critique of a tool for recognizing subtle epeirogenic deformation in modern and ancient settings. *Tectonophysics* 305, 287–306.
- Jankovská V., Chromý P. & Nižniarská M. 2002: “Šafárka” — first palaeobotanical data on vegetation and landscape character of Upper Pleistocene in West Carpathians (North East Slovakia). *Acta Palaeobot.* 42, 1, 29–52.
- Jarvis A., Reuter H.I., Nelson A. & Guevara E. 2008: Hole-filled seamless SRTM data V4, International Centre for Tropical Agriculture (CIAT). Available from <http://srtm.csi.cgiar.org>
- Kinner D.H., Mitášová R., Harmon L., Toma R. & Stallard R. 2005: GIS-based Stream Network Analysis for the Chagres River Basin, Republic of Panama: The Rio Chagres. In: Harmon R. (Ed.): *A multidisciplinary profile of a tropical watershed*. *Springer/Kluwer*, 83–95.
- Kováč M., Hók J., Minár J., Vojtko R., Bielik M., Pipík R., Rakús M., Král J., Šujan M. & Králiková S. 2011: Neogene and Quaternary development of the Turiec Basin and landscape in its catchment: a tentative mass balance model. *Geol. Carpathica* 62, 4, 361–379.
- Lacika J. 1998: Expected changes of arrangement of the valley network in the Poprad catchment. *Geografický Časopis* 50, 3–4, 261–275 (in Slovak with English summary).
- Lang G. 1994: Quartäre Vegetationsgeschichte Europas. *Gustav Fischer Verlag-Jana*, Stuttgart, 1–462.
- Lukniš M. 1964: Remains of older planation surfaces in the Czechoslovak Carpathians. *Geografický Časopis* 16, 3, 289–298 (in Slovak).
- Lukniš M. 1973: Relief of the High Tatra Mts and its surroundings. *Vydav. SAV*, Bratislava, 1–375 (in Slovak).
- Mackin J.H. 1948: Concept of the graded river. *Geol. Soc. Amer. Bull.* 59, 463–512.
- Maglay J., Halouzka R., Baňacký V., Pristaš J. & Janočko J. 1999: Neotectonic map of Slovakia. *GSSR*, Bratislava.
- Mazúr E. 1965: Major features of the West Carpathians in Slovakia as a result of young tectonic movements. In: Mazúr E. (Ed.): *Geomorphological problems of Carpathians*. *SAV*, Bratislava, 9–54.
- Mello J., Filo I., Havrila J., Ivanička J., Madarás J., Maheľ M., Németh Z., Polák M., Pristaš J., Vozár J., Koša E. & Jacko S. Jr. 2000a: Geological map of the Slovenský Raj, Galmus Mts and the Hornád Depression. *Ministry of Environment of Slovak Republic and State Geol. Inst. Dionýz Štúr*, Bratislava.
- Mello J., Filo I., Havrila M., Ivan P., Ivanička J., Madarás J., Németh

- Z., Polák M., Pristaš J., Vozár J., Vozárová A., Liščák P., Kubeš P., Scherer S., Siráňová Z., Szalaiová V. & Žáková E. 2000b: Explanation to geological map of the Slovenský Raj, Galmus Mts and the Hornád Depression (scale 1:50,000). *State Geol. Inst. Dionýz Štúr*, 303 (in Slovak).
- Mello M., Ivanička J., Grecula P., Janočko J., Jacko S. Jr., Elečko M., Pristaš J., Vass D., Polák M., Vozár J., Vozárová A., Hraško Ľ., Kováčik M., Bezák V., Biely A., Németh Z., Kobulský J., Gazdačko Ľ., Madarás J. & Olšavský M. 2008: General geological map of the Slovak Republic, Map sheet: 37-Košice (scale 1:200,000). *Ministry of the Environment of the Slovak Republic, State Geol. Inst. Dionýz Štúr*, Bratislava.
- Mičian Ľ. 1962: Some notes on the Hornád breakthrough in the Stratenká hornatina Mts and morphology of its surroundings. *Geografický Časopis* 14, 1, 57–65 (in Slovak).
- Mitášová H. & Hofierka J. 1993: Interpolation by regularized spline with tension. II. Application to terrain modelling and surface geometry analysis. *Mathematical Geol.* 25, 657–667.
- Mitášová H. & Mitáš Ľ. 1993: Interpolation by regularized spline with tension. I. Theory and implementation. *Mathematical Geol.* 25, 641–655.
- Molin P., Pazzaglia F.J. & Dramis F. 2004: Geomorphic expression of active tectonics in a rapidly deforming forearc, Sila Massif, Calabria, Southern Italy. *Amer. J. Sci.* 304, 559–589.
- Murray A.S. & Wintle A.G. 2000: Luminescence dating of quartz using an improved single-aliquot regenerative dose protocol. *Radiation Measurements* 32, 57–73.
- Olszewska B. & Wiczorek J. 1998: The Paleogene of the Podhale basin (Polish Inner Carpathians) — micropaleontological perspective. *Przegl. Geol.* 46, 721–728.
- Plašienka D. 1999: Tectonochronology and paleotectonic model of the Jurassic-Cretaceous evolution of the Central Western Carpathians. *VEDA Publ.*, Bratislava, 1–125 (in Slovak with English summary).
- Plašienka D., Grecula P., Putiš M., Kováč M. & Hovorka D. 1997: Evolution and structure of the Western Carpathians: an overview. In: Grecula P., Hovorka D. & Putiš M. (Eds.): Geological evolution of the Western Carpathians. *Mineralia Slovaca—Monogr.*, Bratislava, 1–24.
- Polák M., Janočko J., Jacko S. Jr., Potfaj M., Elečko M., Kohút M., Broska I. & Maglay J. 2008: General geological map of the Slovak Republic. Map sheet: 27-Poprad (1:200,000). *Ministry of the Environment of the Slovak Republic, State Geol. Inst. Dionýz Štúr*, Bratislava.
- Preusser F. & Degering D. 2007: Luminescence dating of the Niederweningen mammoth site, Switzerland. *Quat. Int.* 164–165, 106–112.
- Preusser F. & Kasper H.U. 2001: Comparison of dose rate determination using high-resolution gamma spectrometry and inductively coupled plasma-mass spectrometry. *Ancient TL* 19, 17–21.
- Preusser F., Degering D., Fuchs M., Hilgers A., Kadereit A., Klasen N., Krbetschek M., Richter D. & Spencer J.O.G. 2008: Luminescence dating: basics, methods and applications. *E&G Quaternary Science Journal* 57, 1–2, 95–149.
- Preusser F., Chithambo M.L., Götte T., Martini M., Ramseyer K., Sendezera E.J., Susino G.J. & Wintle A.G. 2009: Properties of quartz related to its use as a luminescence dosimeter. *Earth Sci. Rev.* 97, 196–226.
- Roth Z. 1938: Geological structure of the Lučivná area near the Vysoké Tatry Mts. *Rozpravy II. třídy České akademie*, Praha 48, 13, 1–28.
- Ruszkiczay-Rüdiger Zs., Fodor L., Horváth E. & Telbisz T. 2009: Discrimination of fluvial, eolian and neotectonic features in a low hilly landscape: A DEM-based morphotectonic analysis in the Central Pannonian Basin, Hungary. *Geomorphology* 104, 203–217.
- Schumm S.A., Dumont J.F. & Holbrook J.M. 2002: Active tectonics and alluvial rivers. *Cambridge University Press*, Cambridge, 1–276.
- Soták J. 1998: Central Carpathian Paleogene and its constraints. *Slovak Geol. Mag.* 4, 203–211.
- Soták J., Bebej J. & Biroň A. 1996: Detrital analyse of the Paleogene flysch deposits of the Levoča Mts: evidence for sources and paleogeography. *Slovak Geol. Mag.* 2, 3–4, 345–349.
- Soták J., Pereszlényi M., Marschalko R., Milička J. & Starek D. 2001: Sedimentology and hydrocarbon habitat of the submarine fan deposits of the Central Carpathian Paleogene Basin (NE Slovakia). *Mar. Petrol. Geol.* 18, 87–114.
- Steffen D., Preusser F. & Schlunegger F. 2009: OSL quartz age underestimation due to unstable signal components. *Quat. Geochronology* 4, 353–362.
- Vojtko R., Beták J., Hók J., Marko F., Gajdoš V., Rozimant K. & Mojžeš A. 2011: Pliocene to Quaternary tectonics in the Horná Nitra Depression (Western Carpathians). *Geol. Carpathica* 62, 4, 381–393.
- Vozárová A. & Vozár J. 1988: Late Paleozoic in West Carpathians. *Geol. Inst. Dionýz Štúr*, Bratislava, 1–314.
- Wintle A.G. 2008: Luminescence dating: where it has been and where it is going. *Boreas* 37, 471–482.
- Wintle A.G. & Murray A.S. 2006: A review of quartz optically stimulated luminescence characteristics and their relevance in single-aliquot regeneration dating protocols. *Radiation Measurements* 41, 369–391.
- Wobus C., Whipple K.X., Kirby E., Snyder N., Johnson J., Spyropoulou K., Crosby B. & Sheehan D. 2006: Tectonics from topography: Procedure, promise and pitfalls. *Geol. Soc. Amer., Spec. Pap.* 398, 55–74.
- Yeats R.S., Sieh K. & Allen C.R. 1997: The geology of earthquake. *Oxford University Press*, Oxford, 1–568.
- Zander A., Degering D., Preusser F., Kasper H.U. & Brückner H. 2007: Optically stimulated luminescence dating of sublittoral and intertidal sediments from Dubai, UAE: Radioactive disequilibria in the uranium decay series. *Quat. Geochronology* 2, 123–128.
- Zuchiewicz W. 1991: On different approaches to neotectonics: A Polish Carpathians example. *Episodes* 14, 116–124.
- Zuchiewicz W. 1998: Quaternary tectonics of the Outer West Carpathians, Poland. *Tectonophysics* 297, 121–132.